

Advances in Optical Spectroscopy and Imaging of Breast Lesions

Stavros G. Demos · Abby J. Vogel · Amir H. Gandjbakhche

© Springer Science + Business Media, Inc. 2006

Abstract A review is presented of recent advances in optical imaging and spectroscopy and the use of light for addressing breast cancer issues. Spectroscopic techniques offer the means to characterize tissue components and obtain functional information in real time. Three-dimensional optical imaging of the breast using various illumination and signal collection schemes in combination with image reconstruction algorithms may provide a new tool for cancer detection and treatment monitoring.

Keywords Optical imaging · Spectroscopy · Optical mammography · Optical biopsy · Breast imaging · Functional imaging

Abbreviations

MRI	magnetic resonance imaging
NIR	near infrared
FTIR	Fourier transform infrared spectroscopy
NIRA	near infrared autofluorescence
CPLS	cross polarized light scattering
CW	continuous wave
ROC	receiver operating characteristic

AUC	area under curve
RWT	random walk theory
PTB	Physikalisch.-Technische-Bundesanstalt
IDC	invasive ductal carcinoma
TBV	total blood volume
TOAST	temporal optical absorption and scattering tomography
FEM	finite-element model
DOS	diffuse optical spectroscopy
DCE-MRI	dynamic contrast enhanced magnetic resonance imaging
TOI	tissue optical index

Background

According to the National Institutes of Health, breast cancer is the most diagnosed non-skin cancer and the second leading cause of cancer death among women in the United States. Although the breast cancer diagnosis rate has increased, there has been a steady drop in the overall breast cancer death rate since the early 1990s. Depending on the size of the tumor and the involvement of the lymph nodes, survival rates can vary from 45%–95%. The key problem with the breast is the variation in demographic size, texture, chemical composition, and age. X-ray mammography is the gold standard for breast cancer screening and detection. Mammography is most sensitive in women over 35–40 years of age because of their fatty breast composition [1] and less effective and sensitive in younger women because they have denser breasts [2]. For younger women, ultrasound is commonly used. Magnetic resonance imaging (MRI) can also play a significant role in the diagnosis and characterization of breast disease.

According to the National Cancer Institute, up to 10% of all breast cancers, roughly 20,000 cases per year in the

S. G. Demos (✉)
Lawrence Livermore National Laboratory,
7000 East Ave., Livermore, CA 94551, USA
e-mail: demos1@llnl.gov

S. G. Demos
UC Davis Medical School, Medical Center,
2700 Stockton Blvd., Suite 1400,
Sacramento, CA 95817, USA

A. J. Vogel · A. H. Gandjbakhche
Laboratory of Integrative and Medical Biophysics,
National Institutes of Health,
9000 Rockville Pike, Building 9, Room B1E05,
Bethesda, MD 20892, USA

United States are not discovered by X-ray mammography. Also, X-ray mammography uses ionizing radiation and requires uncomfortable breast compression. It also suffers from a significant number of false positives that often lead to unnecessary biopsy, since biopsy is generally required to determine malignancy in most women with an abnormal mammogram. All three techniques, X-ray mammography, ultrasound, and MRI provide high spatial resolution, but comparatively little information about molecular-level changes in breast tissue [1, 3]. Consequently, new detection technologies are needed that can overcome current limitations.

Photonic technology plays an important role in the development of new medical diagnostic and therapeutic instruments. Readily available compact solid-state lasers and various types of light sources allow one to examine tissues in a clinical environment using new and emerging photonic technologies. Major advances in light array detectors provide high signal sensitivities that enable new imaging approaches previously technologically infeasible. In addition, since the computation power of personal computers has been continuously increasing, signal processing speed and image reconstruction algorithms are also advancing. Key benefits of using light for medical imaging are that light is non-ionizing radiation, potentially much cheaper, and can be delivered to a localized region by using either an external source or internally through small optical fibers.

Optical imaging and optical biopsy are two of the research areas where rapid progress has been achieved over the past 10 years. The aim of optical imaging is to provide 3D mapping of tissue structures using light. Photon selection and image reconstruction techniques are implemented to improve image contrast and resolution. Optical biopsy uses the difference in the optical properties of different tissue components to obtain information regarding the tissue makeup, status, and composition. Optical biopsy methods to detect breast cancer *in vivo* have been explored by various research groups. Such optical biopsy methods have demonstrated high sensitivity for cancer detection in various parts of the body. Cancer specific optical ‘signatures’ must be present in order to devise optical biopsy methods for cancer detection. These optical ‘signatures’ may arise from differences in the biochemical and/or structural characteristics of the tissues.

The development of an optical mammography system able to image the breast and detect tumors has been a focus area in the field of optical imaging. Significant progress has been achieved in this very challenging area, and preliminary results have documented the potential of optical imaging for noninvasive breast cancer detection. In recent years, near infrared (NIR) spectroscopy and tomography have been explored by numerous research groups as a means of detecting and characterizing breast cancer. Many groups have demonstrated an ability to accurately quantify

light-tissue interaction properties such as hemoglobin, fat and water absorption and scattering properties, thereby providing valuable functional information. Spatial and temporal contrasts in these properties may be uniquely useful for diagnosing disease.

The objective of this work is to provide a comprehensive review of the progress of photonics methods to address breast cancer issues. This review is divided into two major focus areas: (a) optical spectroscopy methods suitable for tissue evaluation in real time; and (b) noninvasive NIR spectroscopy and imaging for the detection and functional characterization of the tumor.

Optical Biopsy Methods

The term ‘optical biopsy’ describes the use of optical spectroscopy to characterize tissue, and requires direct exposure of the tissue under examination to the light source. Consequently, its application in a clinical setting is best suited for intraoperative use to assist in exploring tissue in real time, or via thin fiberoptic needles that can reach the suspected location within the breast for a minimally invasive evaluation.

The breast is complex; its multiple tissue components make it more difficult to classify using optical spectroscopy than other tissues, e.g., esophagus, colon, bladder, or cervix. However, numerous reports over the past 10 years highlight a number of spectroscopic approaches capable of detecting cancer and characterizing various types of breast tissue components. Within this set of reports, vibrational spectroscopy has been the method of choice for most researchers. This choice may not be surprising given that the vibrational spectra from breast tissue contain a number of peaks arising from a diverse collection of tissue biomolecules.

Vibrational Spectroscopy

The energy spectrum of vibrational modes of tissue biomolecules is typically measured using Raman scattering or Fourier transform infrared spectroscopy (FTIR). However, due to different symmetry selection rules, each technique may be sensitive to a different set of vibrational modes. Both techniques require exposure of the sample to light but the spectral range used by each technique is different. In FTIR, measuring the energy spectrum is direct and involves exposure of the sample to infrared radiation. In Raman scattering, the vibrational spectrum is encoded as the energy difference of the Raman lines from the excitation laser photon energy. Thus, Raman scattering measurements are typically performed using UV or visible lasers, but most often using lasers operating in the NIR spectrum to minimize the background signal arising from tissue autofluorescence.

Early work indicated that substantial biochemical information is imprinted in the Raman scattering spectra of breast tissues, suggesting the potential of this approach for breast cancer diagnosis [4–6]. Redd et al. suggested that the Raman spectra from breast tissue specimens contain features that are attributable to various amounts of carotenoids and lipids [6]. A small contribution from a heme-type signal was detected in some samples of benign breast tissue, and a much stronger heme-type signal was detected in most of the breast cancers. They also reported that the Raman spectra of diseased breast tissue (benign and malignant) exhibit lower contributions from lipids and reduced contributions from carotenoids.

Frank et al. reported through Raman scattering studies with laser wavelengths ranging from 406 to 830 nm that the best defined lipid features were observed with NIR laser excitation, while carotenoid features were strongest in the blue–green spectral range due to resonance enhancement [5]. Extending their work, this same team later reported that the Raman spectra changed dramatically in diseased specimens, with much less evident lipid bands. Moreover, the differences between benign (fibrocystic) and malignant lesions were smaller than those between normal and malignant specimens [4]. These observations were later confirmed when Manoharan et al. asserted the ability of Raman spectroscopy to accurately classify normal, benign, and malignant breast tissues [7].

Raman micro-spectroscopy was more recently used to identify the origin of the peaks observed in the vibrational spectrum from breast tissues. Yu et al. reported that the spectral differences and changes between normal and malignant breast tissue samples could be categorized into the following three groups [8]: (1) The band from the symmetric stretching modes of the PO_2 -group in the DNA shifts from 1,082 to 1,097 cm^{-1} and becomes stronger; this is accompanied by an increase in the intensity of the symmetric stretching modes of O-P-O at 817 cm^{-1} in the RNA. (2) The bands of Amide I and III at 1,657 and 1,273 cm^{-1} change to 1,662 and 1,264 cm^{-1} , respectively, with their intensity and band-widths also increasing. The peak of the C-O stretching modes in the amino acids shifts to higher wave numbers while the intensity of the tryptophan band at 1,368 cm^{-1} diminishes. (3) Fewer Raman bands from lipids are present.

In order to understand the relationship between the Raman spectrum of a sample of breast tissue and its disease state, Shafer–Peltier et al. compared NIR Raman spectroscopic images of human breast tissue specimens (acquired using a confocal microscope) with the corresponding hematoxylin- and eosin-stained images [9]. Spectra obtained from the epithelial cell cytoplasm, cell nucleus, fat, beta-carotene, collagen, calcium hydroxyapatite, calcium oxalate dihydrate, cholesterol-like lipid deposits, and water were used to form a basis of breast tissue spectra. By assuming

that the macroscopically measured Raman spectra were a linear combination of the basis spectra, they developed a chemical/morphological basis to fit the observed features in normal and diseased breast tissues. This model was used to characterize the composition of *ex vivo* specimens and pathologies from 57 patients and predict the disease state [10]. The results indicated that the fit coefficients for fat and collagen were the key parameters in the resulting diagnostic algorithm, which classified samples according to their specific pathological diagnoses, attaining 94% sensitivity and 96% specificity for distinguishing cancerous tissues from normal and benign tissues.

The progress to date using Raman spectroscopy to classify breast tissue specimens provides very encouraging results when considered as a tool to evaluate a localized region via statistical means. It is important to mention that preliminary studies using Fourier transform infrared spectroscopy for the analysis of breast specimens yielded similarly promising results [11, 12]. Dukor et al. reported that benign vs. malignant cells and benign vs. atypical hyperplasia were discriminated with 100% accuracy, and malignant vs. atypical hyperplasia were discriminated with an accuracy of 90% and higher [12]. Ci et al. reported that the spectral differences observed among normal, benign, and malignant breast tissue samples could be categorized by the following [11]: (1) the characteristic spectral patterns of fibroadenoma and carcinoma tissues appear in the frequency regions of 950–1,150 and 2,800–30,50 cm^{-1} respectively; (2) the peak at 970 cm^{-1} is sharper and stronger, and the prominent bands at 1,204, 1,280, and 1,338 cm^{-1} are weaker and broader for carcinoma tissue, whereas the band near 970 cm^{-1} is weaker and the prominent peaks of collagen are sharper and stronger for benign tissue; (3) the band near 1,163 cm^{-1} in benign tissue shifts to 1,171 cm^{-1} in carcinoma tissue; (4) The absorbance (A) ratios of $A(1,032)/A(1,083)$ and $A(2,958)/A(2,853)$ are the lowest in carcinoma tissue and highest in fibroadenoma tissue; and (5) $A(1,459)/A(1,241) > 1.0$ for normal tissue, $A(1,453)/A(1,239) \geq 1.0$ for fibroadenoma, and $A(1,456)/A(1,239) \leq 1.0$ for hyperplasia and carcinoma tissues. Ci et al. concluded that these significant differences revealed the differences in the relative contents of nucleic acids and collagen proteins in breast tissue components. It must be noted that the FTIR measurements discussed above were not obtained directly on the tissue specimens but required extensive tissue processing. Specifically, Ci et al. [11] utilized dehydrated films of cell suspensions extracted from small areas of the specimens. Dukor et al. [12] performed the measurements on the same samples used by pathologists for histopathologic evaluation, i.e., stained samples on plain glass slides. This approach may be a limitation of FTIR spectroscopy that must be resolved prior to its application in a clinical setting.

Light Scattering Methods

The interaction of light with tissue components is dominated by the presence of absorption within the tissue at specific spectral regions and by the optical properties of scattering centers (e.g., nuclei, mitochondrial, membranes). This gives rise to attenuation and changes in the direction of light propagation. The size and shape of the scattering centers affect the scattering cross section differently as a function of wavelength. Consequently, measuring the spectrum of the reflected or transmitted light through tissue provides information about its molecular composition and microscopic structure.

Light scattering spectroscopy methods have been explored by different research groups for their ability to distinguish breast tissue types. Wallon et al. measured the NIR reflectance spectra of 1,100–2,500 nm in specimens from 10 breast cancer patients and found four spectral regions to be different between normal and cancerous tissues: 1,208–1,242, 1,746–1,788, 2,012–2,048 and 2,326–2,368 nm [13]. They also reported that even a minute quantity of cancer infiltration could be detected by NIR spectroscopy.

Yang et al. observed changes on the absorption spectra in the 250–650 nm range of malignant, fibroadenoma, and normal human breast tissues [14–16]. The absorption spectra were extracted from diffuse reflectance measurements and the main differences in absorption were observed at 255–265 and at 275–285 nm. These differences were attributed to changes in proteins and DNA. A set of critical parameters was proposed for separating malignant tissues from fibroadenoma and normal tissues.

Bigio et al. reported on preliminary results of a clinical study designed to test elastic-scattering spectroscopy mediated by fiberoptic probes for transdermal-needle (interstitial) measurements (suitable for a minimally invasive diagnosis) and a hand-held probe (suitable for assessing tumor/resection margins during open surgery) [17]. Preliminary results from *in vivo* measurements on 31 women analyzed using artificial intelligence methods of spectral classification yielded a sensitivity of 69% and specificity of 85%. The authors suggested that they expected these values to improve with the development of more sophisticated data processing algorithms. A fiberoptic needle probe was also used by Van Veen et al. to determine the local optical properties of breast tissue *in vivo* using differential pathlength spectroscopy [18]. This method yields information on the local tissue blood content, the local blood oxygenation, the average micro-vessel diameter, the beta-carotene concentration and the scatter slope. The results showed that malignant breast tissue is characterized by a significant decrease in tissue oxygenation and higher blood content compared to normal breast tissue. These *in vivo* observations may be compared with *ex vivo* measure-

ments reported by Palmer et al. using diffuse reflectance spectroscopy that yielded sensitivity of 30% and specificity of 78% [19]. These significant variations in sensitivity reported by the different groups highlight the importance of developing a common classification algorithm as well as a common measurement scheme for the diagnostic outcome.

Autofluorescence Spectroscopy

There are a large number of biomolecules in tissues that emit light (autofluoresce) under photo-excitation. The most dominant tissue fluorophores are tryptophan, collagen, elastin, NADH, flavoproteins, and porphyrins. Each fluorophore has a distinct absorption and emission spectrum. Similarly to the application of optical spectroscopy for the characterization of organic or inorganic materials, autofluorescence spectroscopy can be used to quantify the relative distribution of the different fluorophores in tissue components for diagnostic purposes.

Pioneering work by Alfano et al. highlighted the potential of autofluorescence spectroscopy for cancer detection [20]. In a paper by Liu et al. [21], Alfano and coworkers explored the use of autofluorescence, Raman scattering and time-resolved light scattering approaches as optical diagnostic techniques to separate diseased and normal breast tissues. Autofluorescence spectroscopic measurements on human breast tissues indicated that the ratio of fluorescence intensity at 340 nm to that at 440 nm could be used to distinguish between cancerous and non-cancerous tissues. Gupta et al. reported on an *in vitro* study involving 63 patients to evaluate autofluorescence spectroscopy under excitation in the near-UV region (nitrogen laser). They reported that significant changes were observed in the spectrally integrated autofluorescence intensity from normal, benign, and cancerous breast tissues. The intensity ratios of cancerous tissues to benign tumor and normal tissues were found to be 3.2 and 2.8, respectively. A discrimination parameter based on spectrally integrated intensity alone provided a sensitivity and specificity up to 99.6%. A similarly high sensitivity was reported by Hage et al. who used laser-induced autofluorescence spectroscopy under 548 nm excitation [23].

The experiments in the paper by Palmer et al. [19] (discussed in the previous section) included characterization of the tissues using autofluorescence spectroscopy under multiple excitation wavelengths in the ultraviolet-visible range. They were successful in discriminating malignant and non-malignant tissues with a sensitivity and specificity of 70% and 92%, respectively [19]. The analysis of the results suggested that the important fluorophores for breast cancer diagnosis are most likely tryptophane, NAD(P)H, and flavoproteins.

Zhang et al. investigated the spectral, polarization, and temporal characteristics of the far-red and near infrared

emission beyond 650 nm of breast tissue specimens under low intensity laser excitation at 532 and 633 nm [24]. The lifetime of this emission was found to be on the order of 1 ns. It was also suggested that the NIR autofluorescence intensity from human breast cancer is different from normal tissue and could potentially be used to detect breast cancer. More recently, Demos et al. reported on results from fresh tissue specimens obtained from surgery that were imaged using NIR autofluorescence under 532 and 633 nm excitation [25]. These images were subsequently compared with the histopathological map of each specimen. The experimental results indicated that the intensity of the NIR emission was considerably different in breast cancer compared to that of the adjacent non-neoplastic tissues (adipose and fibrous tissue). Examples of this approach are shown in Figs. 1 and 2. From the images in Fig. 1, only the NIR fluorescence image under 632.8 nm excitation (Fig. 1b) and the resulting ratio image (Fig. 1d) demonstrate a correlation with cancer identified by histology, with ~1 mm diameter ductal carcinoma areas appearing as features with higher emission. The ratio image (Fig. 1d) improves the visibility and contrast of the cancer and provides sharper delineation of the tumor margins. Table 1 summarizes the average values of the ratio of intensities of cancerous to adipose tissue, cancerous to fibrous tissue, and fibrous to adipose tissue. It was suggested that this method may be suitable for real time detection and imaging of breast cancer lesions in a clinically relevant setting. It was also suggested that 632.8 nm excitation offers key advantages compared to 532 nm excitation for two reasons. First, the images are least affected by blood due to lower

absorption. Second, under 632.8 nm excitation, the autofluorescence intensity ratio between fibrous and cancerous tissue is higher while the ratio of fibrous to adipose tissue is lower compared to the corresponding values under 532 nm excitation. This allows for easier detection (higher contrast) of the cancer in a field of mixed tissue components.

Time-Resolved and Polarization Approaches

Time-resolved and polarization methods are based on measuring the temporal profiles of ultrashort pulses (on the order of a few picoseconds or less) after they propagate through a tissue specimen. Then, information regarding the tissue optical properties can be extracted, which relates to the tissue structure and biochemical composition. This technique can incorporate different laser wavelengths and/or monitoring of the polarization state of the emerging pulse in order to enhance the volume of information.

As discussed in the previous section, Liu et al. suggested the use of time-resolved light scattering for tissue discrimination [21]. This approach was recently employed by Garofalakis et al. to retrieve the reduced scattering coefficients of very thin specimens from time-resolved transmission data [26]. Demos et al. investigated the degree of polarization of the propagating pulse through normal and cancer breast tissue specimens and demonstrated that the intensity, the polarization state, and the temporal profile of the emerging light were different depending on the tissue type [27]. This change in the polarization state is due to the differences in the scattering properties of the tissues.

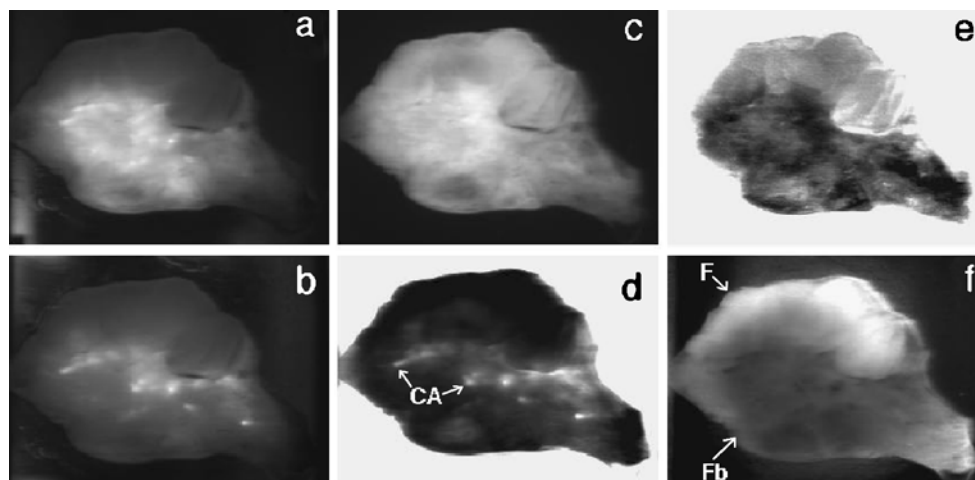


Figure 1 Spectroscopic images of a $\sim 4 \times 3$ cm² human breast tissue, 5 mm thick, with multifocal high grade ductal carcinoma surrounded by fibrous supporting tissue with an adjacent area of fatty infiltration demonstrating enhanced tissue differentiation using NIR light scattering and autofluorescence approaches. NIR autofluorescence (NIRA) images from 700–1,000 nm under laser excitation of (a) 532 and (b)

633 nm. (c) Cross polarized light scattering (CPLS) under 700 nm illumination. (d) Ratio of the 633 nm NIRA image divided by the 700 nm CPLS image. (e) Inter-image ratio of the CPLS image under 1,000 nm illumination divided by the 700 nm CPLS image. (f) Inter-image ratio of the 700 nm CPLS image divided by the 532 nm NIRA image.

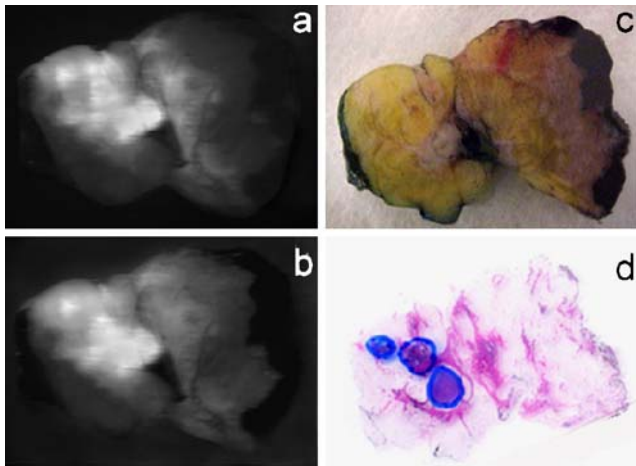


Figure 2 The NIR autofluorescence images of a $\sim 3.2 \times 4.2$ cm² specimen under excitation of (a) 532 nm and (b) 632.8 nm. (c) A color photograph of the same specimen. (d) A contrast-enhanced H & E stained paraffin section of the same specimen with tumor regions outlined with blue marker.

The temporal profile and polarization state of the autofluorescence have also been the focus of preliminary studies. Tadrous et al. used alcohol-fixed tissue samples photoexcited by pulses at 415 nm to acquire fluorescence lifetime images that use fluorescence decay differences between tissue components to generate image contrast [28]. Within individual patients there was a statistically significant difference between benign and malignancy-associated stroma. In addition, benign collagen had a longer decay time than benign epithelium. Mohanty et al. made steady-state measurements of the anisotropy of autofluorescence from malignant and normal breast tissue specimens and reported a dependence of the anisotropy on tissue thickness and type [29].

Spectroscopic Assessment of Lymph Nodes and Microcalcifications

The evaluation and treatment of breast cancer requires establishing whether or not the cancer has spread to the lymph nodes. In response to this issue, Raman and light scattering spectroscopy have been explored as methods that may be able to provide rapid, accurate, and straightforward detection of metastases in the lymph nodes. Johnson et al. discussed the use of light scattering spectroscopy to interrogate excised nodes with pulsed broadband illumination and collection [30]. The study involved specimens from 68 patients, and the analysis of the data suggested 84% sensitivity and 91% specificity in detecting the cancerous nodes. Smith et al. described the use of Raman scattering spectral mapping in the assessment of axillary lymph nodes [31]. This method produced false-color spectral images of lymph node sections representing the

biochemical composition of heterogeneous lymph node features.

Haka et al. demonstrated the use of Raman scattering spectroscopy to characterize microcalcifications in benign and malignant breast lesions [32]. Based on their Raman spectrum, microcalcifications were initially separated into two categories: type I, calcium oxalate dehydrate; and type II, calcium hydroxyapatite. Type I microcalcifications were diagnosed as benign, whereas type II were subdivided into benign and malignant categories using principal component analysis. Using statistical analysis, subtle chemical differences were highlighted in type II that correlated with breast disease. It was suggested that type II microcalcifications that form in benign ducts typically contain a larger amount of calcium carbonate and a smaller amount of protein than those formed in malignant ducts. Using this diagnostic strategy, they were able to distinguish microcalcifications occurring in benign and malignant ducts with a sensitivity of 88% and a specificity of 93%.

Noninvasive Optical Methods

Rationale

Common imaging modalities to diagnose breast cancer are X-ray mammography, computed tomography (CT), and ultrasonography. Much more expensive MRI and PET are sometimes applied to achieve better specificity of the diagnosis (i.e., to separate malignant and benign tissue abnormalities). Optical techniques are considered as potentially much cheaper alternatives for these modalities. In addition, the spectral information about biological tissues embedded in optical techniques can add functional information to simple density imaging. Compared to other available

Table 1 Mean values and standard deviation of the ratio of image intensities from cancer and normal (adipose and fibrous) tissue components as recorded in the NIR autofluorescence images under 532 and 632.8 nm excitation and in the cross-polarized light scattering images under 700 nm illumination.

	Mean value/standard deviation		
	532 nm excitation	632.8 nm excitation	700 nm illumination
Cancer/adipose	2.62/0.67	2.06/0.55	1.21/0.17
Cancer/fibrous	1.34/0.11	1.49/0.27	1.09/0.14
Fibrous/adipose	2.26/0.52	1.30/0.12	1.12/0.20

clinical modalities, optical imaging is able, in principle, to deliver unique spectroscopic information directly related to the physiological status of tissues. Thus, the main goal of optical techniques is to quantify scattering and absorption properties of the breast in 3D at differing wavelengths. Image reconstruction techniques are used to separate the effects of scattering and absorption. Once this separation is realized, multivariate techniques used in standard spectroscopy can provide the concentration of analytes possessing diagnostic value. The most dominant optically active analyte is blood and its major component: hemoglobin.

Studies have indicated that measurements of neovascularity, hypoxia and cellular microenvironments could have a role in tumor detection and treatment planning, as they are all related to tissue function [33–35]. Tumor vessels are distinct from normal vessels: larger in diameter, larger pores in the walls, and lack of contractile properties. Thus, measuring the hemodynamic patterns of tissues, such as blood flow, blood volume, microvascular permeability, and extravascular extracellular space can help to diagnose and manage cancer.

Since breast cancer tissue is mostly hypoxic because of a metabolic imbalance between oxygen supply and consumption [36], measuring it optically has significant potential in diagnosis as well as treatment response. The hemoglobin levels measured by NIR imaging for the normal tissue surrounding the tumor may also be representative of the oxygen carrying capacity of the blood in the breast. Pretreatment hemoglobin levels [37] can also aid in predicting tumor response to primary chemotherapy. Tumor oxygenation may serve to predict its response to radiation treatment, as suggested by its critical role in modifying the dose-response curve [36] and may also be related to the likelihood of occurrence of distant metastases [38]. Vaupel et al. have shown that although hypoxia does not correlate with tumor size, location, grade or stage, it depends critically on whole blood hemoglobin levels [36].

Another important constituent that has diagnostic value is water. Studies have shown that malignant tumors contain much more water than normal breast tissues. However, traditional MRI may not always distinguish between tumor tissue and edema fluid.

Another parameter of significant interest is scattering. Severe scattering of light as it passes through breast tissue causes a great challenge to optical mammography, as it limits the maximum achievable contrast and spatial resolution [39–41]. Optical scattering has been correlated to mammographic density [42], which is a major risk factor for developing cancer [43]. In breast cancer locations, scattering is certainly expected to increase because the tumor cells stimulate endothelial cell proliferation [44], which increases the cellular density. In addition, the tortuous tumor vessel network is held together by dense fibrotic connective tissue [45] that may be optically dense, owing to

the presence of different size scatterers relative to the surrounding tissue. Spectroscopic studies have shown this increase in scattering in a palpable carcinoma [46]. Clinical palpation, although most widely used for gauging tumor response, is a relatively poor non-quantitative predictor of pathological response. Optical methods can show this density change quantitatively.

One of the most promising uses of optical techniques is for women with metastatic lesions, for whom newer therapies (i.e., anti-angiogenic therapy, anti-vascular therapy, immunotherapy, and gene therapy) are currently being studied along with traditional therapy to improve the outcome. In these cases, clinical measurements of tumor response that correlate to outcome are needed to properly evaluate neo-adjuvant therapy. There are currently no non-invasive standard tests that can accurately predict the response of a tumor to therapy.

The unique spectroscopic information provided by optical imaging that directly relates to the physiological status of tissues is currently not being obtained by other available clinical modalities [47]. The fundamental problem with optical methods lies in the turbid interaction of light with biological tissues that prevents embedded inclusions from being spatially resolved with sufficient resolution [48] in a direct optical image. Thus, there are two major challenges for optical imaging: (a) technologies that provide adequate instrumentation; and (b) advances in theory and image reconstruction. To solve the instrumentation challenge, three optical imaging approaches have been developed: time-domain, frequency-domain, and continuous wave (CW). Below, each imaging technique is described followed by relevant research using the imaging technique. Then methods of adding sound to light imaging are described, followed by multimodality imaging techniques, and a discussion of the future of optical imaging for breast cancer tumors.

Time-Domain Optical Imaging

Time-domain optical imaging involves illuminating an object with ultrashort pulses and detecting the pulse that broadens and attenuates as it migrates through the tissue to another surface position located away from the source. A mathematical model of photon migration is then used to fit all or part of the measured temporal distribution of the transmitted light in a number of geometries. This model is used as if it represents a noise-free estimate of the original data, and images are created with the predicted intensities of transmitted pulses. The required instrumentation for time-domain optical imaging includes an expensive pulsed laser source and fast streak cameras or single-photon-counting detecting systems. Time-gating techniques can improve the process, where the total number of photons that

arrive at a detector within a prescribed time window are recovered. Because scattering increases the time-of-flight spent by photons migrating in tissue, the photons that arrive earliest at the detector have encountered the fewest scattering events and deviated least from the direct path between the source and the detector. Accordingly, a spatial intensity image of early-arriving photons can be used to detect tissue regions of high absorbance (e.g., high hemoglobin concentration) based on their attenuation.

An ability to derive parameters such as concentrations of oxygenated and deoxygenated hemoglobin and blood volume from time-resolved optical images of the breast has already been demonstrated [49, 50]. Past approaches of NIR time-gated tomography have suffered from using too few wavelengths and simplistic strategies for spectral deconvolution. More recently there have been significant breakthroughs in the development of algorithms that incorporate multispectral information associated with the different chromophore-specific absorption spectra into the image reconstruction process [41, 42, 51].

Many theoretical constructs have been proposed to analyze experimental data such as using different photon time-of-flight intervals to separate the effects of scattering and absorption. This approach enables one to quantify optical coefficients at different wavelengths as a spectroscopic signature of abnormal tissue embedded in thick, but otherwise normal tissue. The most widely used of these theoretical constructs are diffusion-like models based on the diffusion approximation of the transport equation and models based on the random walk theory (RWT) [52]. These theories can be used to fit experimental data and retrieve optical properties.

Methods currently being pursued generally involve either compressing the breast between two parallel arrays of sources and detectors (or between plates over which individual sources and detectors are scanned) [53–57], or coupling sources and detectors in one or more rings around the surface of the uncompressed breast [39, 58, 59]. The former approach is particularly appropriate for generating single projection images, while the latter is more readily able to yield depth information sufficient for a full 3D image reconstruction.

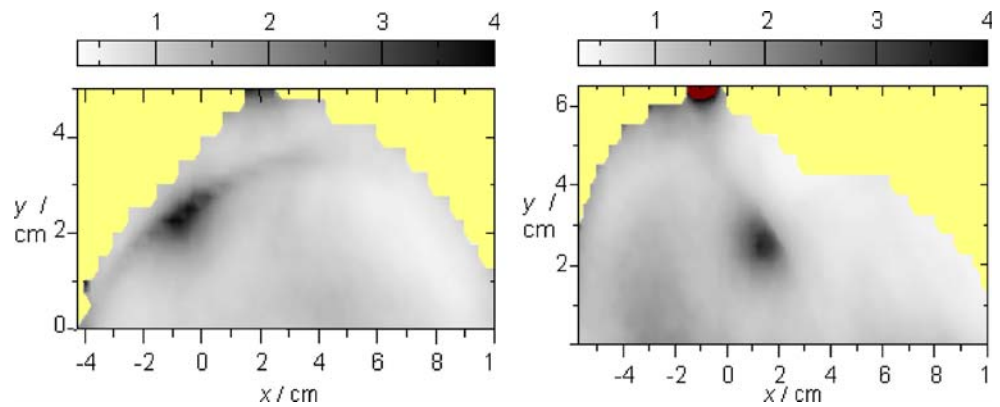
The effect of an inclusion on photon propagation is usually considered either under a perturbation approximation that involves serious restrictions on the inclusion characteristics, or in the frames of RWT, where the influence of increased scattering is modeled by a photon time delay (random walker) proportional to a squared size of the inclusion [60]. Analysis of absorptive abnormalities is expanded beyond the small linear perturbations to the case of larger non-localized targets by introducing an exponential correction factor that depends on the inclusion size and magnitude of absorption perturbation [60, 61].

Rinneberg et al. recorded optical projection mammograms at two wavelengths (670 and 785 nm) using a scanning time-domain instrument [54, 62–64]. From distributions of times of flight of photons through the slightly compressed breast sampled at a large number of scan positions, optical mammograms were generated by various methods of data analysis. In a study of 102 histologically confirmed carcinomas of 154 patients, 72 carcinomas were detected retrospectively in both craniocaudal and medio-lateral projections of the tumor-bearing breast, an additional 20 cases in one projection only, while 10 carcinomas were missed altogether in optical mammograms. Optical properties of each of the 87 tumors identified in optical mammograms were analyzed using the diffraction model of photon density waves, including in the analysis all prior knowledge available. From absorption coefficients at 670 and 785 nm, physiological parameters were deduced. Apart from a few exceptions, they found that the total hemoglobin concentration of tumors exceeded that of healthy breast tissue, whereas blood oxygen saturation was a poor discriminator by itself.

Time-resolved data from the Rinneberg system were used by Gandjbakhche et al. to estimate optical coefficients (absorption and scattering) of the lesion and surrounding normal tissue. Then, physiologically important tissue characteristics, e.g., total blood volume (TBV) and blood oxygenation (S_{O_2}), were obtained from relative concentrations of oxy- and deoxy-hemoglobin, using their known spectral absorptions with *ad hoc* assumptions of constant water content of 30% and an insignificant role of lipids in the tissue absorption at these wavelengths. In some (but not all) cases, the tumors can be seen in the optical images, corresponding to both projections, as illustrated in Fig. 3. Table 2 shows calculated ratios of total blood volume and blood oxygenation of tumors relative to surrounding normal tissue for three patients. Though the sample number is small, these first results give evidence that the malignant tissue in the IDC is hypoxic (in a deoxygenated state) with considerably higher blood volume compared to the surrounding tissue. The latter can be explained by increased vascularization. In another study using time-domain instrumentation with two wavelengths and a water contribution fixed at 30%, lower oxygen saturation was observed in images of two carcinomas [61].

Yates et al. from University College London developed a time-resolved optical tomography system to generate cross-sectional images of the human breast [65]. The 3D breast imaging scheme was based on a 32-channel time-domain imaging system and recorded the temporal distribution of transmitted light at up to 32 locations on the surface simultaneously in response to illumination by picosecond pulses of light at wavelengths of 780 and 815 nm [66]. Images were generated using a reconstruction package

Figure 3 Two-dimensional optical images of the breast, bearing IDC at different projections: (left) craniocaudal and (right) mediolateral.



known as TOAST (temporal optical absorption and scattering tomography), which determines the optical parameters that describe a finite-element model (FEM) of photon migration within an object by comparing its predictions with the measured data [67]. The parameters of the model were then adjusted iteratively to minimize the difference between the two, and thereby 3D images were produced that represented the internal distribution of scatter and absorption [68]. Thirty-eight studies have been performed on 3 healthy volunteers and 21 patients with a variety of breast lesions, including cancer. 17 out of 19 lesions were successfully detected, and optical images of the healthy breast of the same volunteer displayed a heterogeneity that was repeatable over a period of months.

While clinical data are useful to identify overall trends separating malignant from benign disease, the reality may be that separating the two is more complicated. Certain features of benign conditions, such as fibrocystic disease, present difficulties in diagnosing it from cancer, when based only upon mammographic image features [45]. NIR time-resolved tomography is undergoing several clinical trials to evaluate its role in aiding breast lesion diagnosis [46, 69]; however, defining the particular NIR characteristics expected in different types of tumors is not yet well defined.

Frequency-Domain Optical Imaging

Frequency-domain techniques involve illuminating an object with an intensity-modulated beam, and measuring

the AC modulation amplitude, DC intensity and phase shift of the detected signal, typically using a standard heterodyne method. The transport of the modulated beam is often described in terms of the propagation of so-called photon density waves. The phase delay and amplitude attenuation of an intensity wave relative to the incident wave are detected at a point on the tissue surface located some distance away from its source. When the photon density waves encounter tissue regions of varying optical properties, they refract, scatter, and interfere, as any other wave. Hence these waves, when incident on a light-absorbing heterogeneity within a tissue, can ‘reflect’ and distort the propagating photon density wave as well as to other ‘reflected’ waves. The result is a perturbation in the measured phase delay and amplitude attenuation whose magnitude is dependent on the location, size and optical contrast of heterogeneities within a tissue volume. Measurements of phase delay and amplitude attenuation are then used to reconstruct an interior optical property map.

Tromberg et al. designed a handheld frequency-domain system and observed a decrease in oxygen saturation in spectroscopic studies on a palpable mass diagnosed as ductal carcinoma *in situ* [46]. In a related study that monitored neoadjuvant chemotherapy using spectroscopy, initial tissue oxygen saturation was found to be lower in the lesion compared to the surrounding tissue followed by a slight peak, when tracked over 10 weeks of treatment [70]. Heffer et al. [56] used an ‘oxygenation index’ generated from frequency-domain measurements to show a decrease in oxygen saturation in carcinomas.

In previous work at Dartmouth College, McBride et al. [71] used a frequency-domain NIR tomography system to image a subject with a 2.5 cm IDC. Although an increase in hemoglobin was observed, a reduction in oxygen saturation was not found. Dehghani et al. [42] used 3D modeling to obtain tomographic images from a patient with IDC and reported an increase in blood oxygen saturation level, contrary to expectation.

Srinivasan [72] used multi-wavelength NIR tomography to noninvasively quantify physiological parameters of breast

Table 2 Calculated ratios of total blood volume and blood oxygenation for three subjects.

Age	Tumor size (mm)	TBV(tumor) / TBV(tissue)	SO ₂ (tumor) / SO ₂ (tissue)
84	25×15×15	1.8	0.77
57	40×35×30	2.0	0.90
52	15×15×15	2.1	0.80

tumors using direct spectral reconstruction. Frequency domain NIR measurements were incorporated with a new spectrally constrained direct chromophore and scattering image reconstruction algorithm, which was validated in simulations and experimental phantoms. Images of total hemoglobin, oxygen saturation, water and scatter were obtained with higher accuracy than previously reported. Three of six cases studied were malignant (infiltrating ductal carcinomas) and showed higher hemoglobin (34%–86), a reduction in oxygen saturation, an increase in water content as well as scatter changes relative to surrounding normal tissue. Three of the six cases were benign, two of which were diagnosed with fibrocystic disease and showed a dominant contrast in water, consistent with fluid-filled cysts. Scatter amplitude was the main source of contrast in the volunteer with the benign fibrosis, which typically contains denser collagen tissue. The changes monitored correspond to physiological changes associated with angiogenesis, hypoxia, and cell proliferation anticipated in cancers. These changes represent potential diagnostic indicators, which can be assessed to characterize breast tumors. The physiological changes observed can be extended to monitoring response to therapy and predicting risk of malignancy or aggressiveness of tumors. NIR tomography is an imaging method that can directly quantify some functional processes noninvasively.

CW Optical Imaging

CW optical imaging systems require a source that either emits at a constant intensity, or is modulated at a low frequency (a few kHz) in order to exploit the significant improvements in sensitivity available from phase-locked detection techniques. The constant intensity source is focused on the tissue surface and the tissue volume is illuminated with light whose intensity becomes exponentially attenuated with distance from the tissue surface. Measurements of the intensity of light transmitted between two points on the surface of tissue are not only relatively straightforward and inexpensive to obtain, but also contain a remarkable amount of useful information. The presence of diseased tissue may be characterized by wavelength-dependent light absorption or scattering properties. From the wavelength-dependent attenuation of light collected at the tissue surface, an interior map of the tissue optical properties can be determined. In highly scattering media such as tissue, photons can take one of many different paths from a source to a detector. The CW techniques have difficulty detecting the distribution of the photon path lengths, they are limited in the amount of information they can provide for imaging of interior optical properties. However, the instrumentation is much simpler than the time- and frequency-domain instrumentation because much

cheaper light sources and detectors can be used and the acquisition time is an order of magnitude faster.

Chance et al. developed a NIR method capable of rapidly acquiring data from the breast with a handheld puck [73]. The CW device was used to measure tumor hemoglobin and hemoglobin desaturation compared to the mirror image site on the contralateral normal breast. They found an increased hemoglobin concentration due to angiogenesis and decreased hemoglobin saturation due to hyper-metabolism of the cancer in the cancerous breast compared to the normal breast. Receiver Operating Characteristic (ROC) evaluation of the nomogram showed 95% in the area under the curve (AUC) for 116 patients with tumor sizes down to and including those of 0.8–1 cm in diameter.

Conover et al. acquired NIR spectroscopic measurements *in vivo* on subcutaneous rat mammary adenocarcinomas and showed through sensitivity and specificity analyses that NIR spectroscopy imaging may identify clinically relevant hypoxia, even when its spatial extent is below the resolution limit of the NIR spectroscopy technique [74].

Simick et al. used NIR transillumination spectroscopy to show that optical spectroscopy predicted the radiological assessment of density with a principal component analysis model in the range of 90% with an odds ratio comparable to mammography [75]. Parameters such as oxygen saturation, water fraction, and scattering provided fundamental metabolic information about tissue that is not currently being obtained with any other imaging modality.

Adding Sound to Optical Imaging

Laser opto-acoustic imaging may help to overcome the problem of pure optical imaging associated with the loss of sensitivity and resolution due to strong light scattering. Acousto-optical tomography (AOT), also called ultrasound-modulated optical technique, is based on the ultrasonic modulation of coherent laser light in biological tissue. The modulated component of the speckle pattern carries spatial information determined by the ultrasound and can be utilized for tomographic imaging. Three possible mechanisms have been identified for the ultrasonic modulation of light in scattering media [76].

The first mechanism is based on ultrasound-induced variations of the optical properties of the media. As an ultrasonic wave propagates in a scattering medium, the medium is compressed and rarified depending on location and time. Variations of density cause the optical properties of the medium—including the absorption coefficient, the scattering coefficient, and the index of refraction—to vary. Accordingly, the detected intensity of light varies with the ultrasonic wave. The second mechanism is based on

variations of the optical phase in response to ultrasound-induced displacements of scatterers. The displacements of scatterers, assumed to follow ultrasonic amplitudes, modulate the physical path lengths of light traversing through the ultrasonic field. Multiply scattered light accumulates modulated physical path lengths along its path. Consequently, the intensity of the speckles formed by the multiply scattered light fluctuates with the ultrasonic wave. The third mechanism is based on variations of the optical phase in response to ultrasonic modulation of the index of refraction. As a result of ultrasonic modulation of the index of refraction, the optical phase between two consecutive scattering events is modulated. As in the second mechanism, multiply scattered light accumulates modulated phases along its path, and the modulated phase causes the intensity of the speckles formed by the multiply scattered light to vary with the ultrasonic wave.

Photo-acoustic tomography (PAT) in biological tissues, also called opto-acoustic or thermo-acoustic tomography, is another ultrasound-mediated biophotonic imaging modality. In PAT, a short-pulsed electromagnetic source (i.e., laser) is used to irradiate the tissue samples. The photo-acoustic waves excited by thermoelastic expansion are measured around the sample by wideband ultrasonic transducers, which are sensitive to small vibrations. The electromagnetic heating must be rapid to produce photoacoustic waves efficiently; in other words, static temperature distribution or slow heating does not produce photo-acoustic waves effectively. The acquired photoacoustic waves then are used to deduce the electromagnetic absorption distribution. Regardless of whether a laser source or a radiofrequency source is used, the data collection and image reconstruction are conducted in the same way. The key task in PAT is to determine the electromagnetic absorption distribution from the measured photoacoustic data; i.e., to map the electromagnetic absorption heterogeneity of the tissue. One straightforward approach is to use focused ultrasonic transducers to localize the photo-acoustic sources in linear or sector scans and then construct the images directly from the data. An alternative method is to use wideband unfocused detectors to acquire photo-acoustic data and then reconstruct the electromagnetic absorption distribution.

Multimodality Techniques

The unique features of optical methods, including their high sensitivity for detecting photons and use of non-ionizing radiation, render optical imaging a technology that could complement existing breast imaging techniques for cancer detection and characterization. The compatibility of the technology with most other radiological imaging techniques allows the creation of combined modalities for simultaneous breast examinations that yield a superior feature set.

Furthermore, optical methods are economic and can acquire data continuously; hence, they may be used for real-time monitoring.

Optical methods are intrinsically sensitive to blood, water, and lipid, the main analytes of breast tissue. They measure tissue composition, information that is qualitatively different, but complementary, to that of the structural images provided by mammography and ultrasound. In addition, optical methods are able to quantify oxygenated hemoglobin and deoxygenated hemoglobin. Thus, hemoglobin oxygen saturation levels determined by this method are direct and absolute, albeit at low resolution.

Since the spatial resolution of optical tomography is limited by scattering, multi-modality imaging is increasingly being used to interrogate tissue morphology and function simultaneously because of the inherently optimized co-registration. Structure and function of tissue afford different physical bases for contrast, and combinations have proven beneficial in the diagnosis and management of disease [77].

To date, NIR techniques have been combined with several high spatial resolution, structure-specific imaging modalities, including X-ray tomosynthesis [55], ultrasound [71, 78], and MRI [79–81], to study human tissues and small animals. Past experiences have contributed to a variety of imaging systems, imaging geometries, and numerical reconstruction techniques, but have not led to a consensus on the optimal way of applying *a priori* derived constraints.

Adjunctive noninvasive imaging modalities are often needed to characterize suspicious abnormalities, especially in women with radiographically dense breasts. There is considerable potential for functional NIR imaging to help distinguish breast cancer noninvasively, yet this modality has consistently suffered from low spatial resolution. Such hybrid approaches could generate image data that combine the functional information of optical imaging with the high spatial resolution of structural information in MRI. Hybrid imaging systems also avoid complications associated with tissue movement between separate exams, which reduce co-registration accuracy and thus degrade the diagnostic value of the image fusion [82].

In addition to co-registration, data sets from combined NIR and MRI imaging offer other synergistic benefits, namely anatomical priors (from high spatial resolution MRI) enhance NIR (i.e., high contrast resolution) image reconstruction. NIR spectroscopy is biochemically rich, but spectroscopic imaging is hindered by the highly scattered photon paths that reduce resolution in tissue [49]. The most widely adopted approach to this problem incorporates parameter estimation strategies based on models of light propagation in tissue. The estimation task is sensitive to small perturbations in the light measurements, not all of which are caused by the intrinsic changes in tissue optical

properties. Experience has shown that significant improvements in the stability and accuracy of the reconstruction process can be obtained by including prior anatomical/optical information [51, 55, 58, 83–85].

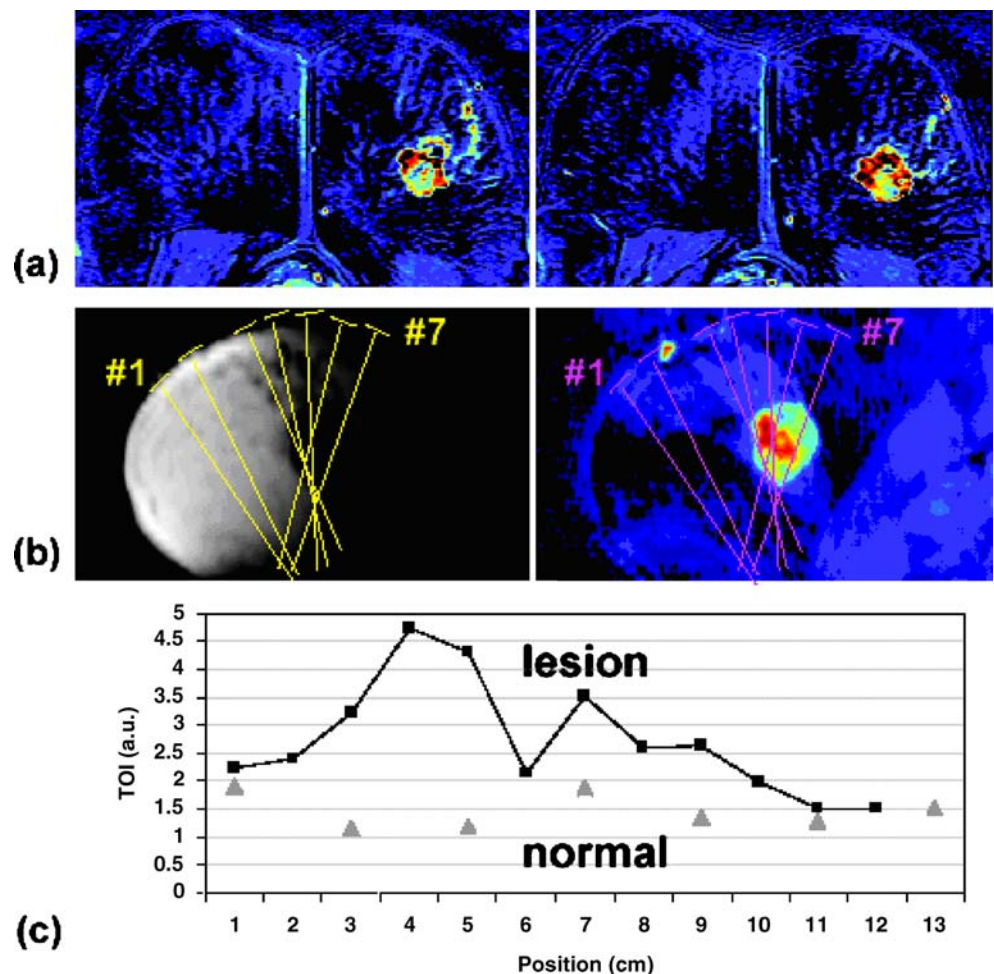
Techniques for incorporating this information are relatively new, and are the subject of active research in a variety of disciplines, including medical imaging [80, 86, 87], industrial process imaging [88], and geophysical surveying [89], yet there is no clear consensus on the optimal approach.

Brooksby et al. [90] used NIR tomography and magnetic resonance imaging (MRI) on a healthy woman *in vivo*. The NIR image reconstruction technique implemented the MR structure as an input parameter. The algorithm incorporated the MR spatially segmented regions into a regularization matrix that linked locations with similar MR properties. This reconstruction algorithm allowed maximal flexibility upon use with *a priori* data, and was validated on a series of tissue-like breast phantoms. Spatially resolved images of absorption and reduced scattering coefficients at multiple wavelengths (660–850 nm) were used to estimate values of

hemoglobin concentration, oxygen saturation, water fraction, scattering power, and scattering amplitude within adipose and glandular breast tissue types identified from MRI. Dramatic changes in spatial property distributions arose when the MRI was used to guide these reconstructions. Glandular tissue was observed to have more than four times the water than adipose tissue, and almost twice as much blood volume, as well as slightly reduced oxygen saturation.

Hsiang et al. [91] developed a handheld scanning probe based on broadband diffuse optical spectroscopy (DOS) in combination with dynamic contrast enhanced MRI (DCE-MRI) to quantitatively characterize locally-advanced breast cancers in six patients. Measurements were performed sequentially using external fiducial markers for co-registration, as seen in Fig. 4. Lesion patterns were categorized according to MRI morphological data, and 3D DCE-MRI slices were converted into a volumetric matrix with isotropic voxels to generate views that coincided with the DOS scanning plane. Lesion volume and depth at each DOS measurement site were determined, and a tissue

Figure 4 (a) The original enhancement maps from two slices (4 mm thick) demonstrate an unenhanced necrotic center in the lesion. (b) The re-sliced pre-contrast image along the seven DOS markers demonstrating a hypointense mass, and the corresponding enhancement map demonstrating a strongly enhanced mass. These images are 1.5 cm thick, and do not show the necrotic core. (c) The tissue optical index curve measured at each DOS location from the lesion and the normal breast tissues in the contralateral breast. A dip is seen at 6 cm in the DOS scan line, likely due to the necrotic core.



optical index (TOI) that reflects both angiogenic and stromal characteristics was derived from broadband DOS data.

Future Trend: Molecular Imaging

There may be instances in which intrinsic spectroscopic signatures of tissue are not sufficient for detection of disease. This can occur when the specific disease results in only very small changes to the tissue's scattering and absorption properties, or when the scattering and absorption properties are not unique to the tissue abnormality under investigation. In such cases, an exogenous source of optical contrast, such as a fluorescing contrast agent is required to detect and locate the disease. The presence of extrinsic fluorescent molecules in tissues can provide useful contrast mechanisms. The concentration of these exogenous fluorophores in the body can be related to functional and metabolic activities, and therefore to the disease processes. A desired feature of such contrast agent is to absorb and emit light in the NIR spectral region when light propagation through tissue is maximized, thus optimizing the excitation efficiency and minimizing signal loss.

Fluorescent dyes that target specific tumor receptors [92], or that are activated and fluoresce by tumor-associated enzymes (such as cathepsins and matrix metalloproteinases) [93], have been shown to identify their molecular targets *in vivo*. The latter probes probably hold the greatest promise, because they are quenched in the absence of the targeted enzymatic activity, yielding highly specific fluorescence signals.

The basic principles behind fluorescence-enhanced NIR optical tomography are focused on the kinetics of the fluorescence generation. When a molecule of significant aromaticity absorbs light corresponding to a transitional energy level, it becomes activated into a 'singlet' state from where it can relax radiatively, releasing light of lower energy (or higher wavelength) than the incident light. Typically, the fluorescence lifetime, or the mean time that the fluorophore is in the activated 'singlet' state, is mediated by the local environment impacting the relative rates of radiative and nonradiative decay to the ground state.

Fluorescence-enhanced NIR imaging is accomplished when the propagating excitation light activates exogenous fluorescent agents within the tissue. The generated fluorescent light propagates through the tissue to its surface and can be detected or imaged using appropriate instrumentation after rejecting the excitation light or other unwanted signal components. Typically, the greater the ratio of exogenous fluorescent agent in the tissue volume of interest to that in the surrounding tissue, the greater the contrast for image reconstruction. However, in the case of time-dependent measurements, it is the kinetics that create a nanosecond or

sub-nanosecond time-delay between absorption or excitation light and generation of fluorescent light that provides additional contrast for imaging.

Selected molecular activity can be achieved with high sensitivity when the background fluorescence is quenched. Also, this method offers increased signal sensitivity so that cancers could be detected at their molecular onset, before anatomic changes become apparent. Therefore, therapies can be initiated at a very early stage, which is the single most important strategy in achieving high survival rates. In addition, specific cancer parameters such as growth kinetics, angiogenesis growth factors, tumor cell markers, and genetic alterations could be studied without perturbing the tumor environment. Finally, this additional information could aid in the development of novel targeted drugs and therapies, and could allow assessment of their efficacy at the molecular level. The importance of this imaging strategy is further amplified by considering that photon technology can detect single photons, so that it can resolve fluorescent molecules at nanomolar to picomolar concentrations, and requires instrumentation that is of relatively low cost and that uses non-ionizing radiation.

Because the fluorescent decay of a given probe can be affected by pH, oxygenation, free ion concentrations, glucose, or other analytes, it can provide an optical assessment of analytes not otherwise directly measurable. Furthermore, fluorescence may be used as a probe to measure environmental conditions in a particular locality by capitalizing on changes in fluorophore lifetimes [94, 95]. Ratiometric dyes have been used to measure the pH of tissues using multiwavelength CW techniques. Oxygen sensitive fluorescing contrast agents have also been developed to provide noninvasive measurement of tissue oxygen status. Because fluorescence lifetimes can be directly measured using the time- and frequency-domain approaches, a quantitative assessment of the analyte concentration can also be obtained independently from the concentration of the molecular probe, or fluorophore. In addition to fluorescence lifetime, the quantum efficiency, or the amount of fluorescence light generated per unit light absorbed can also be assessed using CW techniques.

As a result, an exceptional level of specificity is now possible due to the advances in the design of exogenous markers. Molecules can now be tailor-made to bind only to specific receptor sites in the body. These receptor sites may be antibodies or other biologically interesting molecules. Fluorophores may be bound to these engineered molecules and injected into the body, where they preferentially concentrate at specific sites of interest [96, 97]. The advent of nanoparticles has opened an exciting opportunity for such molecular imaging.

Breast imaging is an excellent frontier in which to develop fluorescence contrast-enhanced optical tomography

owing to the large volume of tissue and the urgent need for diagnostic measures in patients with breast cancer. Although researchers are tackling the problems of NIR fluorescence-enhanced contrast imaging, the clinical applications of agents for diagnostic breast imaging are already emerging. The translation to diagnostic detection of metastases of other cancers may be forthcoming.

Discussion

The histological examination of breast tissue is currently performed by selecting one of the well-developed invasive breast biopsy techniques (i.e., excisional biopsy, axillary node dissection, sentinel node dissection, or fine needle aspiration), depending on the location, size, palpability, and characteristics of the abnormality. Breast excisions remain one of the most common surgical operations for diagnosing and treating breast cancer. In the current setting, while frozen section analysis is available, there are technical limitations to cutting certain types of tissue and as a result, immediate histological analysis is not possible or practical. Therefore, developing technology that can offer detection and delineation of tumor margins in real time may be very useful to a surgeon during a diagnostic or therapeutic procedure.

The progress to date in using various optical spectroscopy methods for the classification of breast tissue arguably provides a solid foundation for the development of spectroscopy-based instrumentation for real time pathological assessment. Most of the approaches use single point measurement techniques that interrogate a small volume of tissue at each measurement. As mentioned earlier, the potential role of this technology in addressing clinical needs related to breast cancer detection and treatment may be for intraoperative tissue characterization in real time or via designing thin fiberoptic needles to reach the suspected location within the breast for an evaluation of a suspected lesion. Such 'optical needle biopsies' have recently been designed and preliminary *in vivo* results are encouraging [17, 98]. Similar work is also in progress by other research teams [99].

Point spectroscopic measurements or spectral imaging may be used to detect a tumor or establish tumor margins in real time in the operating room. Without a tissue diagnosis to determine the borders of a tumor before a breast lumpectomy, it is estimated that 40%–70% of margins will be malignant. Optical biopsy methods could be most useful to detect nonpalpable or very small lesions and therefore guide the surgeon.

Although the development of optical mammography as a means of routine screening for early incidence of breast cancer in asymptomatic women is not universally regarded as an achievable goal, several applications have been identified for which the technique may be beneficial for

specific patients. It has recently been proposed that NIR imaging may be useful for prescreening younger women to identify those at increased risk of developing disease [49]. The facility to study tissue function, such as the oxygenation status of hemoglobin, may also make optical imaging a potent tool for detecting responses to new and existing forms of therapy [70]. A further potential application of NIR imaging is to assess and monitor surrounding healthy tissues after treatment.

Acknowledgments The authors acknowledge the following agencies for support of their research in breast cancer: The California Breast Cancer Research Program and the Center for Biophotonics, an NSF Science and Technology Center, managed by the University of California, Davis, under Cooperative Agreement No. PHY 0120999. This work was performed in part at Lawrence Livermore National Laboratory under the auspices of the U.S. Department of Energy under Contract W-7405-Eng-48. This work was supported by the Intramural Program of the National Institutes of Health, National Institute of Child Health and Human Development.

References

1. Carney PA, Kasales CJ, Tosteson ANA, Weiss JE, Goodrich ME, Poplack SP, et al. Likelihood of additional work-up among women undergoing routine screening mammography: the impact of age, breast density, and hormone therapy use. *Prev Med* 2004;39(1):48–55.
2. Hindle WH, Davis LWD, Wright D. Clinical value of mammography for symptomatic women 35 years of age and younger. *Am J Obstet Gynecol* 1999;180(6 Pt 1):1484–90.
3. Hata T, Takahashi H, Watanabe K, Takahashi M, Taguchi K, Itoh T, et al. Magnetic resonance imaging for preoperative evaluation of breast cancer: a comparative study with mammography and ultrasonography. *J Am Coll Surg* 2004;198(2):190–7.
4. Frank C, McCreery R, Redd D. Raman-spectroscopy of normal and diseased human breast tissues. *Anal Chem* 1995;67 5:777–83.
5. Frank C, Redd D, Gansler T, McCreery R. Characterization of human breast specimens with near-IR Raman spectroscopy. *Anal Chem* 1994;66(3):319–26.
6. Redd D, Feng Z, Yue K, Gansler T. Raman-spectroscopic characterization of human breast tissues—implications for breast-cancer diagnosis. *Appl Spectrosc* 1993;46(6):787–91.
7. Manoharan R, Shafer K, Perelman L, Wu J, Chen K, Deinum G, et al. Raman spectroscopy and fluorescence photon migration for breast cancer diagnosis and imaging. *Photochem Photobiol* 1998;67:15–22.
8. Yu G, Xu X, Niu Y, Wang B, Song Z, Zhang C. Studies on human breast cancer tissues with Raman microspectroscopy. *Spectroscopy and Spectral Analysis* 2004;24(11):1359–62.
9. Shafer-Peltier K, Haka A, Fitzmaurice M, Crowe J, Myles J, Dasari R, et al. Raman microspectroscopic model of human breast tissue: implications for breast cancer diagnosis *in vivo*. *J Raman Spectrosc* 2002;33(7):552–63.
10. Haka A, Shafer-Peltier K, Fitzmaurice M, Crowe J, Dasari R, Feld M. Diagnosing breast cancer by using Raman spectroscopy. *Proc Natl Acad Sci U S A* 2005;102(35):12371–6.

11. Ci Y, Gao T, Feng J, Guo Z. Fourier transform infrared spectroscopic characterization of human breast tissue: implications for breast cancer diagnosis. *Applied Spectrosc* 1999;53 (3):312–5.
12. Dukor R, Liebman M, Johnson B. A new, non-destructive method for analysis of clinical samples with FT-IR microspectroscopy. *Breast cancer tissue as an example. Cell Mol Biol* 1998;44 (1): 211–7.
13. Wallon J, Yan S, Tong J, Meurens M, Haot J. Identification of breast carcinomatous tissue by near-infrared reflectance spectroscopy. *Applied Spectroscopy* 1994;48 (2):190–3.
14. Yang Y, Celmer E, Koutcher J, Alfano R. UV reflectance spectroscopy probes DNA and protein changes in human breast tissues. *J Clin Laser Med Surg* 2001;19 (1):35–9.
15. Yang Y, Celmer E, Koutcher J, Alfano RR. DNA and protein changes caused by disease in human breast tissues probed by the Kubelka–Munk spectral function. *Photochem Photobiol* 2002;75 (6):627–32.
16. Yang Y, Katz A, Celmer E, Zurawska-Szczepaniak M, Alfano R. Fundamental differences of excitation spectrum between malignant and benign breast tissues. *Photochem Photobiol* 1997;66 (4):518–22.
17. Bigio I, Bown S, Briggs G, Kelley C, Lakhani S, Pickard D, et al. Diagnosis of breast cancer using elastic-scattering spectroscopy: preliminary clinical results. *J Biomed Opt* 2000;5 (2):221–8.
18. Van Veen R, Amelink A, Menke-Pluymers M, Van der Pol C, Sterenborg HJ. Optical biopsy of breast tissue using differential path-length spectroscopy. *Phys Med Biol* 2005;50 (11):2573–81.
19. Palmer G, Zhu C, Breslin T, Xu F, Gilchrist K, Ramanujam N. Comparison of multiexcitation fluorescence and diffuse reflectance spectroscopy for the diagnosis of breast cancer. *IEEE Trans Biomed Eng* 2003;50 (11):1233–42.
20. Alfano RR, Tata D, Cordero J, Tomashefsky P, Longo F, Alfano M. Laser-induced fluorescence spectroscopy from native cancerous and normal tissue. *IEEE J Quantum Electron* 1984;20 (12):1507–11.
21. Liu C, Das B, Glassman W, Tang G, Yoo KM, Zhu H, et al. Raman, fluorescence, and time-resolved light-scattering as optical diagnostic-techniques to separate diseased and normal biomedical media. *J Photochem Photobiol B Biol* 1992;16 (2):187–209.
22. Gupta P, Majumder S, Uppal A. Breast cancer diagnosis using N2 laser excited autofluorescence spectroscopy. *Lasers Surg Med* 1997;21 (5):417–22.
23. Hage R, Galhanone P, Zangaro R, Rodrigues K, Pacheco M, Martin A, et al. Using the laser-induced fluorescence spectroscopy in the differentiation between normal and neoplastic human breast tissue. *Lasers Med Sci* 2003;18 (3):171–6.
24. Zhang G, Demos S, Alfano R. Far-red and NIR spectral wing emission from tissues under 532 nm and 632 nm photo-excitation. *Lasers Life Sci* 1999;9:1–16.
25. Demos S, Bold R, deVere White R, Ramsamooj R. Investigation of near infrared autofluorescence imaging for the detection of breast cancer. *IEEE J Sel Top Quantum Electron* 2005;11 (4):791–98.
26. Garofalakis A, Zacharakis G, Filippidis G, Sanidas E, Tsiftsis D, Stathopoulos E, et al. Optical characterization of thin female breast biopsies based on the reduced scattering coefficient. *Phys Med Biol* 2005;50 (11):2583–96.
27. Demos S, Savage H, Heerdt A, Schantz S, Alfano R. Time resolved degree of polarization for human breast tissue. *Opt Commun* 1996;124:439–42.
28. Tadrous P, Siegel J, French PM, Shousha S, Lalani E, Stamp G. Fluorescence lifetime imaging of unstained tissues: early results in human breast cancer. *J Pathol* 2003;199 (3):309–17.
29. Mohanty SK, Ghosh N, Majumder SK, Gupta PK. Depolarization of autofluorescence from malignant and normal human breast tissues. *Appl Opt* 2001;40 (7):1147–54.
30. Johnson K, Chicken DW, Pickard D, Lee A, Briggs G, Falzon M, et al. Elastic scattering spectroscopy for intraoperative determination of sentinel lymph node status in the breast. *J Biomed Opt* 2004;9 (6):1122–28.
31. Smith J, Kendall C, Sammon A, Christie-Brown J, Stone N. Raman spectral mapping in the assessment of axillary lymph nodes in breast cancer. *Technol Cancer Res Treat* 2003;2 (4): 327–31.
32. Haka A, Shafer-Peltier K, Fitzmaurice M, Crowe J, Dasari R, Feld MS. Identifying microcalcifications in benign and malignant breast lesions by probing differences in their chemical composition using Raman spectroscopy. *Cancer Res* 2002;62 (18):5375–80.
33. Boudreau N, Myers C. Breast cancer-induced angiogenesis: multiple mechanisms and the role of the microenvironment. *Breast Cancer Res* 2003;5 (3):140–6.
34. Vaupel P, Hockel M. Blood supply, oxygenation status and metabolic microenvironment of breast cancers: characterization and therapeutic relevance. *Int J Oncol* 2000;17 (5):869–79.
35. Williams K, Cowen R, Stratford I. Hypoxia and oxidative stress. Tumour hypoxia-therapeutic considerations. *Breast Cancer Res* 2001;3 (5):328–31.
36. Vaupel P, Kallinowski F, Okunieff P. Blood flow, oxygen and nutrient supply, and metabolic microenvironment of human tumors : a review. *Cancer Res* 1989;49:6449–65.
37. Bottini A, Berruti A, Brizzi MP, Bersiga A, Generali D, Allevi G, et al. Pretreatment haemoglobin levels significantly predict the tumour response to primary chemotherapy in human breast cancer. *Br J Cancer* 2003;89 (6):977–82.
38. Brizel DM, Scully SP, Harrelson JM, Layfield LJ, Bean JM, Prosnitz LR, et al. Tumor oxygenation predicts for the likelihood of distant metastases in human soft tissue sarcoma. *Cancer Res* 1996;56:941–3.
39. Dehghani H, Pogue BW, Poplack SP, Paulsen KD. Multiwave-length three-dimensional near-infrared tomography of the breast: initial simulation, phantom, and clinical results. *Appl Opt* 2003;42 (1):135–45.
40. Hattery D, Chernomordik V, Loew M, Gannot I, Gandjbakhche AH. Analytical solutions for time-resolved fluorescence lifetime imaging in a turbid medium such as tissue. *JOSA A* 2001; 18:1523.
41. Li A, Zhang Q, Culver JP, Miller EL, Boas DA. Reconstructing chromosphere concentration images directly by continuous-wave diffuse optical tomography. *Opt Lett* 2004;29 (3):256–8.
42. Srinivasan S, Pogue BW, Jiang S, Dehghani H, Kogel C, Soho S, et al. Interpreting hemoglobin and water concentration, oxygen saturation, and scattering measured *in vivo* by near-infrared breast tomography. *Proc Natl Acad Sci U S A* 2003;100 (21):12349–54.
43. Mandelson MT, Oestreicher N, Porter PL, White D, Finder CA, Taplin SH, et al. Breast density as a predictor of mammographic detection: comparison of interval- and screen-detected cancers. *J Natl Cancer Inst* 2000;92 (13):1081–7.
44. Kuszysk BS, Corl FM, Franano FN, Bluemke DA, Hofmann LV, Fortman BJ, Fishman EK. Tumor transport physiology: implications for imaging and image-guided therapy. *AJR Am J Roentgenol* 2001;177:747–53.
45. Thomsen S, Tatman D. Physiological and pathological factors of human breast disease that can influence optical diagnosis. *Ann N Y Acad Sci* 1998;838:171–93.
46. Tromberg BJ, Shah N, Lanning R, Cerussi A, Espinoza J, Pham T, et al. Non-invasive *in vivo* characterization of breast tumors using photon migration spectroscopy. *Neoplasia* 2000;2 (1):26–40.
47. Gandjbakhche A. (2001). Diffused optical imaging and spectroscopy, *in vivo*. *C R Acad Sci Ser IV*:1073–79.
48. Gandjbakhche AH, Nossal R, Bonner RF. Resolution limits for optical transillumination of abnormalities deeply embedded in tissues. *Med Phys* 1994;21:185–91.
49. Pogue B, Jiang S, Dehghani H, Kogel C, Soho S, Srinivasan S, et al. Characterization of hemoglobin, water, and NIR scattering in breast tissue: analysis of intersubject variability and menstrual cycle changes. *J Biomed Opt* 2004;9:541–52.
50. Torricelli A, Spinelli L, Pifferi A, Taroni P, Cubeddu R, Danesini G. Use of a nonlinear perturbation approach for *in vivo* breast

- lesion characterization by multi-wavelength time-resolved optical mammography. *Opt Express* 2003;11:853–967.
51. Corlu A, Choe R, Durduran T, Lee K, Schweiger M, Arridge SR, et al. Diffuse optical tomography with spectral constraints and wavelength optimization. *Appl Opt* 2005;44 (11):2082–93.
 52. Hebden JC, Yates TD, Gibson A, Everdell N, Arridge SR, Chicken DW, et al. Monitoring recovery after laser surgery of the breast with optical tomography: a case study. *Appl Opt* 2005;44:1898–904.
 53. Culver JP, Choe R, Holboke MJ, Zubkov L, Durduran T, Slemper A, et al. Three-dimensional diffuse optical tomography in the parallel plane transmission geometry: evaluation of a hybrid frequency domain/continuous wave clinical system for breast imaging. *Med Phys* 2003;30 (2):235–47.
 54. Grosenick D, Moesta KT, Wabnitz H, Mucke J, Stroszczynski C, Macdonald R, et al. Time-domain optical mammography: initial clinical results on detection and characterization of breast tumors. *Appl Opt* 2003;42 (3):170–86.
 55. Li A, Miller EL, Kilmer ME, Brukilacchio TJ, Chaves T, Stott J, et al. Tomographic optical breast imaging guided by three-dimensional mammography. *Appl Opt* 2003;42:5181–90.
 56. Pera VE, Heffer EL, Siebold H, Schütz O, Heywang-Köbrunner S, Götz L, et al. Spatial second derivative image processing: an application to optical mammography to enhance the detection of breast tumors. *J Biomed Opt* 2003;8:517–24.
 57. Taroni P, Danesini G, Torricelli A, Pifferi A, Spinelli L, Cubeddu R. Clinical trial of time-resolved scanning optical mammography at 4 wavelengths between 683 and 975 nm. *J Biomed Opt* 2004;9 (3):464–73.
 58. Barbour RL, Schmitz CH, Klemer DP, Pei Y, Graber HL. Design and initial testing of system for simultaneous dynamic optical tomographic mammography. In: *Biomedical Optics Topical Meetings*, 2004. Washington, DC: Optical Society of America; 2004. p. WD4.
 59. Jiang H, Xu Y, Iftimia N, Eggert J, Klove K, Baron L, et al. Three-dimensional optical tomographic imaging of breast in a human subject *IEEE Trans. Med Imag* 2001;20:1334–40.
 60. Chernomordik V, Hattery D, Pifferi A, Taroni P, Torricelli A, Valentini G, et al. A random walk methodology for quantification of the optical characteristics of abnormalities embedded within tissue-like phantoms. *Opt Lett* 2000;25:951.
 61. Chernomordik V, Hattery DW, Grosenick D, Wabnitz H, Rinneberg H, Moesta KT, et al. Quantification of optical properties of a breast tumor using random walk theory. *J Biomed Opt* 2002;7 (1):80–7.
 62. Rinneberg H, Grosenick D, Moesta KT, Mucke J, Gebauer B, Stroszczynski C, et al. Scanning time-domain optical mammography: detection and characterization of breast tumors *in vivo*. *Technol Cancer Res Treat* 2005;4 (5):483–96.
 63. Grosenick D, Wabnitz H, Moesta KT, Mucke J, Moller M, Stroszczynski C, et al. Concentration and oxygen saturation of haemoglobin of 50 breast tumours determined by time-domain optical mammography. *Phys Med Biol* 2004;49 (7):1165–81.
 64. Grosenick D, Wabnitz H, Rinneberg HH, Moesta KT, Schlag PM. Development of a time-domain optical mammograph and first *in vivo* applications. *Appl Opt* 1999;38 (13):2927–43.
 65. Yates T, Hebden JC, Gibson A, Everdell N, Arridge SR, Douek M. Optical tomography of the breast using a multi-channel time-resolved imager. *Phys Med Biol* 2005;50:2503–17.
 66. Schmidt F, Fry M, Hillman E, Hebden J, Delpy D. A 32-channel time-resolved instrument for medical optical tomography. *Rev Sci Instrum* 2000;71:256–65.
 67. Arridge SR, Schweiger M. Image reconstruction in optical tomography. *Philos Trans R Soc Lond Ser B Biol Sci* 1997;352 (1354):717–26.
 68. Arridge S, Hebden J, Schweiger M, Schmidt F, Fry M, Hillman E, et al. A method for 3D time-resolved optical tomography. *Int J Imaging Syst Technol* 2000;11:2–11.
 69. McBride TO, Pogue BW, Jiang J, Österberg UL, Paulsen KD. A parallel-detection frequency-domain near infrared tomography system for hemoglobin imaging of the breast *in vivo*. *Rev Sci Instrum* 2001;72:1817–24.
 70. Jakubowski DB, Cerussi AE, Bevilacqua F, Shah N, Hsiang D, Butler J, et al. Monitoring neoadjuvant chemotherapy in breast cancer using quantitative diffuse optical spectroscopy: a case study. *J Biomed Opt* 2004;9 (1):230–8.
 71. Pogue BW, Zhu H, Nwaigwe C, McBride TO, Osterberg UL, Paulsen KD, et al. Hemoglobin imaging with hybrid magnetic resonance and near-infrared diffuse tomography. *Adv Exp Med Biol* 2003;530:215–24.
 72. Srinivasan S, Pogue BW, Brooksby B, Jiang S, Dehghani H, Kogel C, et al. Near-infrared characterization of breast tumors *in-vivo* using spectrally-constrained reconstruction. *Technol Cancer Res Treat* 2005;4 (5):513–26.
 73. Chance B, Nioka S, Zhang J, Conant EF, Hwang E, Briest S, et al. Breast cancer detection based on incremental biochemical and physiological properties of breast cancers: a six-year, two-site study. *Acad Radiol* 2005;12 (8):925–33.
 74. Conover DL, Fenton BM, Foster TH, Hull EL. An evaluation of near infrared spectroscopy and cryospectrophotometry estimates of haemoglobin oxygen saturation in a rodent mammary tumour model. *Phys Med Biol* 2000;45 (9):2685–700.
 75. Simick MK, Jong R, Wilson B, Lilge L. Non-ionizing near-infrared radiation transillumination spectroscopy for breast tissue density and assessment of breast cancer risk. *J Biomed Opt* 2004;9 (4):794–803.
 76. Wang LV. Ultrasound-mediated biophotonic imaging: a review of acousto-optical tomography and photo-acoustic tomography. *Dis Markers* 2004;19:123–38.
 77. Conti PS, Lilien DL, Hawley K, Keppler J, Grafton ST, Bading JR. PET and [18F]-FDG in oncology: a clinical update. *Nucl Med Biol* 1996;23:717.
 78. Zhu Q, Huang M, Chen N, Zarfes K, Jagjivan B, Kane M, et al. Ultrasound-guided optical tomographic imaging of malignant and benign breast lesions: initial clinical results of 19 cases. *Neoplasia* 2003;5 3:379–88.
 79. Gulsen G, Yu H, Wang J, Nalcioğlu O, Merritt S, Bevilacqua F, et al. Congruent MRI and near-infrared spectroscopy for functional and structural imaging of tumors. *Technol Cancer Res Treat* 2002;1 (6):497–505.
 80. Ntziachristos V, Yodanis AG, Schnall MD, Chance B. MRI-guided diffuse optical spectroscopy of malignant and benign breast lesions. *Neoplasia* 2002;4:347.
 81. Vishwanath K, Pogue B, Mycek MA. Quantitative fluorescence lifetime spectroscopy in turbid media: comparison of theoretical, experimental and computational methods. *Phys Med Biol* 2002;47 (18):3387–405.
 82. Goertzen AL, Meadors AK, Silverman RW, Cherry SR. Simultaneous molecular and anatomical imaging of the mouse *in vivo*. *Phys Med Biol* 2002;47:4315.
 83. Pogue BW, Paulsen KD. High-resolution near-infrared tomographic imaging simulations of the rat cranium by use of a priori magnetic resonance imaging structural information. *Opt Lett* 1998;23:1716.
 84. Vauhkonen M, Vadasz D, Kaipio JP, Somersalo E, Karjalainen PA. Tikhonov regularization and prior information in electrical impedance tomography. *IEEE Trans Med Imag* 1998;17:285.
 85. Borsic A, Lionheart WRB, McLeod CN. Generation of anisotropic-smoothness regularization filters for EIT. *IEEE Trans Med Imag* 2002;21:579.
 86. Ouyang X, Wong WH, Johnson VE, Hu X, Chen C. Incorporation of correlated structural images in PET image reconstruction. *IEEE Trans Med Imag* 1994;13:627.

87. Glidewell M, Ng KT. Anatomically constrained electrical impedance tomography for anisotropic bodies via a two-step approach. *IEEE Trans Med Imag* 1995;14:498.
88. Dickin F, Wang M. Electrical resistance tomography for process tomography. *Meas Sci Technol* 1996;7:247.
89. Loke MH. (1997). Electrical imaging surveys for environmental and engineering studies.
90. Brooksby B, Jiang S, Dehghani H, Pogue BW, Paulsen KD, Weaver J, et al. Combining near infrared tomography and magnetic resonance imaging to study *in vivo* breast tissue: implementation of a Laplacian-type regularization to incorporate MR structure. *J Biomed Opt* 2005;10(5):51504.
91. Hsiang D, Shah N, Yu H, Su M, Cerussi A, Butler J, et al. Coregistration of dynamic contrast enhanced MRI and broadband diffuse optical spectroscopy for characterizing breast cancer. *Technol Cancer Res Treat* 2005;4(5):549–58.
92. Achilefu S, Dorshow RB, Bugaj JE, Rajagopalan R. Novel receptor-targeted fluorescent contrast agents for *in vivo* tumor imaging. *Invest Radiol* 2000;35(8):479–85.
93. Weissleder R, Tung C, Mahmood U, Bogdanov A. *In vivo* imaging of tumors with protease-activated near-infrared fluorescent probes. *Nat Biotechnol* 1999;17:375–8.
94. Hutchinson CL, Lakowicz JR, Sevickmuraca EM. Fluorescence lifetime-based sensing in tissues—a computational study. *Biophys J* 1995;68(4):1574–82.
95. Mordon S, Devoisselle JM, Maunoury V. *In-vivo* pH measurement and imaging of tumor-tissue using a pH-sensitive fluorescent-probe (5,6-carboxyfluorescein)—instrumental and experimental studies. *Photochem Photobiol* 1994;60(3):274–9.
96. Weissleder R. A clearer vision for *in vivo* imaging. *Nat Biotechnol* 2001;19(4):316–17.
97. Kamalov VF, Struganova IA, Yoshihara K. Temperature dependent radiative lifetime of J-aggregates. *J Phys Chem* 1996;100:8640.
98. Andrews R, Mah R, Da Silva L. The NASA smart probe project for real-time multiple-microsensor tissue recognition. *SPIE Proceedings* 2004;5326:92–7.
99. Zhu C, Labawy C, Burnside E, Harter J, Ramanujam N. (2005). Development of optical sensor for spectroscopic detection of breast cancer during needle biopsy. *Lasers Surg Med* 6(6 15 Suppl. 17).